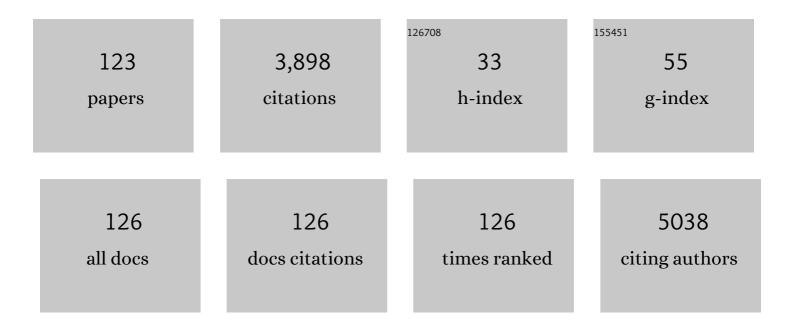


List of Publications by Year in descending order

Source: https://exaly.com/author-pdf/4633927/publications.pdf Version: 2024-02-01



YIANG LI

| # | Article | IF | CITATIONS |
|----|---|------|-----------|
| 1 | Co–Ferrocene MOF/Glucose Oxidase as Cascade Nanozyme for Effective Tumor Therapy. Advanced Functional Materials, 2020, 30, 1910085. | 7.8 | 283 |
| 2 | Synergistic thermoradiotherapy based on PEGylated Cu 3 BiS 3 ternary semiconductor nanorods with strong absorption in the second near-infrared window. Biomaterials, 2017, 112, 164-175. | 5.7 | 153 |
| 3 | Facile synthesis of single-crystalline mesoporous α-Fe2O3 and Fe3O4 nanorods as anode materials for lithium-ion batteries. Journal of Materials Chemistry, 2012, 22, 20566. | 6.7 | 148 |
| 4 | Platinum Nanoparticles to Enable Electrodynamic Therapy for Effective Cancer Treatment. Advanced Materials, 2019, 31, e1806803. | 11.1 | 130 |
| 5 | Microneedle Coating Techniques for Transdermal Drug Delivery. Pharmaceutics, 2015, 7, 486-502. | 2.0 | 115 |
| 6 | FeS@BSA Nanoclusters to Enable H ₂ Sâ€Amplified ROSâ€Based Therapy with MRI Guidance. Advanced Science, 2020, 7, 1903512. | 5.6 | 114 |
| 7 | One Stone Two Birds: Zr-Fc Metal–Organic Framework Nanosheet for Synergistic Photothermal and Chemodynamic Cancer Therapy. ACS Applied Materials & Interfaces, 2020, 12, 20321-20330. | 4.0 | 105 |
| 8 | Porous Pt Nanospheres Incorporated with GOx to Enable Synergistic Oxygenâ€Inductive Starvation/Electrodynamic Tumor Therapy. Advanced Science, 2020, 7, 2001223. | 5.6 | 93 |
| 9 | ZnS@BSA Nanoclusters Potentiate Efficacy of Cancer Immunotherapy. Advanced Materials, 2021, 33, e2104037. | 11.1 | 89 |
| 10 | Upconversion Composite Nanoparticles for Tumor Hypoxia Modulation and Enhanced Near-Infrared-Triggered Photodynamic Therapy. ACS Applied Materials & Interfaces, 2018, 10, 15494-15503. | 4.0 | 86 |
| 11 | Selfâ€Templated Synthesis of Singleâ€Crystal and Singleâ€Domain Ferroelectric Nanoplates. Angewandte Chemie - International Edition, 2012, 51, 9283-9287. | 7.2 | 76 |
| 12 | Porous Pt nanoparticles loaded with doxorubicin to enable synergistic Chemo-/Electrodynamic Therapy. Biomaterials, 2020, 255, 120202. | 5.7 | 73 |
| 13 | Ultrathin Anatase TiO ₂ Nanosheets for Highâ€Performance Photocatalytic Hydrogen Production. Small, 2017, 13, 1604115. | 5.2 | 72 |
| 14 | Multifunctional metal-organic framework-based nanoreactor for starvation/oxidation improved indoleamine 2,3-dioxygenase-blockade tumor immunotherapy. Nature Communications, 2022, 13, 2688. | 5.8 | 70 |
| 15 | Phage-based vaccines. Advanced Drug Delivery Reviews, 2019, 145, 40-56. | 6.6 | 68 |
| 16 | Cu–Ferroceneâ€Functionalized CaO ₂ Nanoparticles to Enable Tumorâ€Specific Synergistic Therapy with GSH Depletion and Calcium Overload. Advanced Science, 2021, 8, e2100241. | 5.6 | 68 |
| 17 | Nitrofurazone-loaded electrospun PLLA/sericin-based dual-layer fiber mats for wound dressing applications. RSC Advances, 2015, 5, 16940-16949. | 1.7 | 57 |
| 18 | Bismuth embedded silica nanoparticles loaded with autophagy suppressant to promote photothermal therapy. Biomaterials, 2019, 221, 119419. | 5.7 | 54 |

XIANG LI

| # | Article | IF | CITATIONS |
|----|--|-----|-----------|
| 19 | ZnS@ZIF-8 core-shell nanoparticles incorporated with ICG and TPZ to enable H ₂ S-amplified synergistic therapy. Theranostics, 2020, 10, 7671-7682. | 4.6 | 53 |
| 20 | Multifunctional Electrospun Nanofibers for Enhancing Localized Cancer Treatment. Small, 2018, 14, e1801183. | 5.2 | 52 |
| 21 | Polarization-dependent epitaxial growth and photocatalytic performance of ferroelectric oxide heterostructures. Nano Energy, 2018, 45, 304-310. | 8.2 | 50 |
| 22 | Novel patterning of nano-bioceramics: template-assisted electrohydrodynamic atomization spraying. Journal of the Royal Society Interface, 2008, 5, 253-257. | 1.5 | 48 |
| 23 | Electrodeposition of silver nanoparticle arrays on ITO coated glass and their application as reproducible surface-enhanced Raman scattering substrate. Applied Surface Science, 2011, 258, 1831-1835. | 3.1 | 45 |
| 24 | Mesoporous silica nanoparticles with manipulated microstructures for drug delivery. Colloids and Surfaces B: Biointerfaces, 2012, 95, 274-278. | 2.5 | 45 |
| 25 | A Fibrous Localized Drug Delivery Platform with NIR-Triggered and Optically Monitored Drug Release. Langmuir, 2016, 32, 9083-9090. | 1.6 | 45 |
| 26 | Development and characterisation of cellulose based electrospun mats for buccal delivery of non-steroidal anti-inflammatory drug (NSAID). European Journal of Pharmaceutical Sciences, 2017, 102, 147-155. | 1.9 | 44 |
| 27 | Monodispersed LiFePO4@C core–shell nanostructures for a high power Li-ion battery cathode. Journal of Power Sources, 2014, 246, 696-702. | 4.0 | 43 |
| 28 | Mesopores induced zero thermal expansion in single-crystal ferroelectrics. Nature Communications, 2018, 9, 1638. | 5.8 | 43 |
| 29 | Ferric Hydroxide-Modified Upconversion Nanoparticles for 808 nm NIR-Triggered Synergetic Tumor Therapy with Hypoxia Modulation. ACS Applied Materials & Interfaces, 2019, 11, 385-393. | 4.0 | 43 |
| 30 | Mesoporous silica decorated with platinum nanoparticles for drug delivery and synergistic electrodynamic-chemotherapy. Nano Research, 2020, 13, 2209-2215. | 5.8 | 42 |
| 31 | Fenton/Fenton-like metal-based nanomaterials combine with oxidase for synergistic tumor therapy. Journal of Nanobiotechnology, 2021, 19, 325. | 4.2 | 42 |
| 32 | Fe3O4@Pt nanoparticles to enable combinational electrodynamic/chemodynamic therapy. Journal of Nanobiotechnology, 2021, 19, 206. | 4.2 | 38 |
| 33 | A novel jet-based nano-hydroxyapatite patterning technique for osteoblast guidance. Journal of the Royal Society Interface, 2010, 7, 189-197. | 1.5 | 35 |
| 34 | Tunable photoluminescence properties of well-aligned ZnO nanorod array by oxygen plasma post-treatment. Applied Surface Science, 2014, 289, 252-256. | 3.1 | 35 |
| 35 | Upconversion nanocrystal â€~armoured' silica fibres with superior photoluminescence for miRNA detection. Chemical Communications, 2018, 54, 6324-6327. | 2.2 | 35 |
| 36 | Multifunctional MoO2-ICG nanoplatform for 808nm-mediated synergetic photodynamic/photothermal therapy. Applied Materials Today, 2019, 15, 472-481. | 2.3 | 35 |

Xiang Li

| # | Article | IF | CITATIONS |
|----|--|------|-----------|
| 37 | Tailoring of textured transparent conductive SnO2:F thin films. Journal of Alloys and Compounds, 2013, 574, 427-431. | 2.8 | 34 |
| 38 | Near-infrared luminescent CaTiO ₃ :Nd ³⁺ nanofibers with tunable and trackable drug release kinetics. Journal of Materials Chemistry B, 2015, 3, 7449-7456. | 2.9 | 34 |
| 39 | Luminescent CaTiO ₃ :Yb,Er nanofibers co-conjugated with Rose Bengal and gold nanorods for potential synergistic photodynamic/photothermal therapy. Journal of Materials Chemistry B, 2017, 5, 5128-5136. | 2.9 | 32 |
| 40 | Development of nano-hydroxyapatite coating by electrohydrodynamic atomization spraying. Journal of Materials Science: Materials in Medicine, 2008, 19, 1545-1551. | 1.7 | 31 |
| 41 | Microstructural and functional stability of large-scale SnO2:F thin film with micro-nano structure. Journal of Alloys and Compounds, 2013, 550, 144-149. | 2.8 | 30 |
| 42 | Phase-Modified Up-Conversion Luminescence in Er-Doped Single-Crystal PbTiO ₃ Nanofibers. Journal of Physical Chemistry C, 2014, 118, 5486-5493. | 1.5 | 28 |
| 43 | Production of a fluorescence resonance energy transfer (FRET) biosensor membrane for microRNA detection. Journal of Materials Chemistry B, 2017, 5, 7133-7139. | 2.9 | 28 |
| 44 | A Dual-Color Luminescent Localized Drug Delivery System with Ratiometric-Monitored Doxorubicin Release Functionalities. ACS Biomaterials Science and Engineering, 2016, 2, 652-661. | 2.6 | 27 |
| 45 | Octahedral-shaped perovskite nanocrystals and their visible-light photocatalytic activity. Chemical Communications, 2014, 50, 6027-6030. | 2.2 | 26 |
| 46 | Hollow ferric-tannic acid nanocapsules with sustained O ₂ and ROS induction for synergistic tumor therapy. Biomaterials Science, 2020, 8, 3844-3855. | 2.6 | 26 |
| 47 | Novel preparation and characterization of porous alginate films. Carbohydrate Polymers, 2010, 79, 989-997. | 5.1 | 25 |
| 48 | pH-Triggered SrTiO ₃ :Er Nanofibers with Optically Monitored and Controlled Drug Delivery Functionality. ACS Applied Materials & Interfaces, 2015, 7, 25514-25521. | 4.0 | 25 |
| 49 | Sizeâ€Controlled Singleâ€Crystal Perovskite PbTiO ₃ Nanofibers from Edgeâ€Shared TiO ₆ Octahedron Columns. Small, 2012, 8, 2959-2963. | 5.2 | 24 |
| 50 | Gold nanorod-assembled ZnGa ₂ O ₄ :Cr nanofibers for LED-amplified gene silencing in cancer cells. Nanoscale, 2018, 10, 13432-13442. | 2.8 | 24 |
| 51 | Silica nanofibers with controlled mesoporous structure via electrospinning: From random to orientated. Materials Letters, 2013, 94, 100-103. | 1.3 | 23 |
| 52 | Crystallization and concentration modulated tunable upconversion luminescence of Er ³⁺ doped PZT nanofibers. Journal of Materials Chemistry C, 2015, 3, 382-389. | 2.7 | 23 |
| 53 | Synthesis of porous CaTiO3 nanotubes with tunable hollow structures via single-nozzle electrospinning. Materials Letters, 2015, 152, 82-85. | 1.3 | 23 |
| 54 | Electrostatic Force–Driven Oxide Heteroepitaxy for Interface Control. Advanced Materials, 2018, 30, e1707017. | 11.1 | 23 |

Xiang Li

| # | Article | IF | CITATIONS |
|----|---|-----|-----------|
| 55 | Electrohydrodynamic deposition of nanotitanium doped hydroxyapatite coating for medical and dental applications. Journal of Materials Science: Materials in Medicine, 2011, 22, 491-496. | 1.7 | 22 |
| 56 | Delivery of amino acid oxidase <i>via</i> catalytic nanocapsules to enable effective tumor inhibition. Journal of Materials Chemistry B, 2020, 8, 8546-8557. | 2.9 | 22 |
| 57 | A feasible approach toward bioactive glass nanofibers with tunable protein release kinetics for bone scaffolds. Colloids and Surfaces B: Biointerfaces, 2014, 122, 785-791. | 2.5 | 20 |
| 58 | Facile synthesis and visible photocatalytic activity of single-crystal TiO ₂ /PbTiO ₃ heterostructured nanofiber composites. CrystEngComm, 2015, 17, 1024-1029. | 1.3 | 20 |
| 59 | Single-crystal nanofibers of Zr-doped new structured PbTiO3: hydrothermal synthesis, characterization and phase transformation. Journal of Materials Chemistry, 2011, 21, 3562. | 6.7 | 19 |
| 60 | Selective Deposition of Silver Oxide on Singleâ€Domain Ferroelectric Nanoplates and Their Efficient Visibleâ€Light Photoactivity. Chemistry - A European Journal, 2016, 22, 12160-12165. | 1.7 | 19 |
| 61 | A Multifunctional Nanocrystalline CaF ₂ :Tm,Yb@mSiO ₂ System for Dualâ€īriggered and Optically Monitored Doxorubicin Delivery. Particle and Particle Systems Characterization, 2016, 33, 896-905. | 1.2 | 19 |
| 62 | Rare-earth-doped upconversion nanocrystals embedded mesoporous silica nanoparticles for multiple microRNA detection. Chemical Engineering Journal, 2019, 374, 863-869. | 6.6 | 19 |
| 63 | Polarization-Modified Upconversion Luminescence in Er-Doped Single-Crystal Perovskite PbTiO ₃ Nanofibers. Journal of Physical Chemistry C, 2015, 119, 17326-17333. | 1.5 | 18 |
| 64 | Ethylene glycol (EG) solvothermal synthesis of flower-like LiMnPO ₄ nanostructures self-assembled with (010) nanobelts for Li-ion battery positive cathodes. CrystEngComm, 2016, 18, 3282-3288. | 1.3 | 18 |
| 65 | Enhanced cell uptake of fluorescent drug-loaded nanoparticles via an implantable photothermal fibrous patch for more effective cancer cell killing. Journal of Materials Chemistry B, 2017, 5, 7504-7511. | 2.9 | 18 |
| 66 | Sulfiteâ€Inserted MgAl Layered Double Hydroxides Loaded with Glucose Oxidase to Enable SO ₂ â€Mediated Synergistic Tumor Therapy. Advanced Functional Materials, 2021, 31, 2103262. | 7.8 | 18 |
| 67 | Electrospray deposition of nanohydroxyapatite coatings: A strategy to mimic bone apatite mineral. Thin Solid Films, 2011, 519, 2328-2331. | 0.8 | 17 |
| 68 | Fabrication and characterization of size-controlled single-crystal-like PZT nanofibers by sol–gel based electrospinning. Journal of Alloys and Compounds, 2013, 579, 617-621. | 2.8 | 17 |
| 69 | Optically Monitoring Mineralization and Demineralization on Photoluminescent Bioactive Nanofibers. Langmuir, 2016, 32, 3226-3233. | 1.6 | 17 |
| 70 | Fibrous CaF2:Yb,Er@SiO2-PAA â€~tumor patch' with NIR-triggered and trackable DOX release. Materials and Design, 2017, 119, 85-92. | 3.3 | 16 |
| 71 | Implantable composite fibres with Self-supplied H2O2 for localized chemodynamic therapy. Chemical Engineering Journal, 2020, 388, 124211. | 6.6 | 16 |
| 72 | Single-Crystal BiFeO ₃ Nanoplates with Robust Antiferromagnetism. ACS Applied Materials & Interfaces, 2018, 10, 5785-5792. | 4.0 | 15 |

XIANG LI

| # | Article | lF | CITATIONS |
|----|--|-----|-----------|
| 73 | Implantable fibrous scaffold with hierarchical microstructure for the â€~on-site' synergistic cancer therapy. Chemical Engineering Journal, 2020, 402, 126204. | 6.6 | 15 |
| 74 | ATP-responsive hollow nanocapsules for DOX/GOx delivery to enable tumor inhibition with suppressed P-glycoprotein. Nano Research, 2021, 14, 222-231. | 5.8 | 15 |
| 75 | Polymersome Nanoreactorâ€Mediated Combination Chemodynamicâ€Immunotherapy via ROS Production and Enhanced STING Activation. Advanced Therapeutics, 2021, 4, 2100130. | 1.6 | 15 |
| 76 | α-Fe2O3@Pt heterostructure particles to enable sonodynamic therapy with self-supplied O2 and imaging-guidance. Journal of Nanobiotechnology, 2021, 19, 358. | 4.2 | 15 |
| 77 | Effect of glass tempering on microstructure and functional properties of SnO2:F thin film prepared by atmosphere pressure chemical vapor deposition. Thin Solid Films, 2013, 544, 357-361. | 0.8 | 14 |
| 78 | Improved mechanical properties of SnO2:F thin film by structural modification. Ceramics International, 2014, 40, 2557-2564. | 2.3 | 14 |
| 79 | Pre-perovskite nanofiber: a new direct-band gap semiconductor with green and near infrared photoluminescence. RSC Advances, 2013, 3, 5453. | 1.7 | 13 |
| 80 | Growth and Bending-Sensitive Photoluminescence of a Flexible PbTiO ₃ /ZnO Nanocomposite. ACS Applied Materials & Interfaces, 2014, 6, 10935-10940. | 4.0 | 13 |
| 81 | A facile approach to upconversion crystalline CaF ₂ :Yb ³⁺ ,Tm ³⁺ @mSiO ₂ nanospheres for tumor therapy. RSC Advances, 2016, 6, 38365-38370. | 1.7 | 13 |
| 82 | Implantable fibrous â€~patch' enabling preclinical chemo-photothermal tumor therapy. Colloids and Surfaces B: Biointerfaces, 2020, 192, 111005. | 2.5 | 13 |
| 83 | Hydrothermal synthesis of ferroelectric PbTiO3 nanoparticles with dominant {001} facets by titanate nanostructure. CrystEngComm, 2013, 15, 8036. | 1.3 | 12 |
| 84 | Facile synthesis of PbTiO3 truncated octahedra via solid-state reaction and their application in low-temperature CO oxidation by loading Pt nanoparticles. Journal of Materials Chemistry A, 2014, 2, 9035-9039. | 5.2 | 12 |
| 85 | Platinum–copper alloy nanoparticles armored with chloride ion transporter to promote electro-driven tumor inhibition. Bioactive Materials, 2022, 12, 143-152. | 8.6 | 12 |
| 86 | An electrically driven jetting technique for diverse high-resolution surface structures of nanometre hydroxyapatite crystals. Colloids and Surfaces B: Biointerfaces, 2011, 82, 562-570. | 2.5 | 11 |
| 87 | Synthesis of CaTiO ₃ Nanofibers with Controllable Drugâ€Release Kinetics. European Journal of Inorganic Chemistry, 2015, 2015, 4532-4538. | 1.0 | 11 |
| 88 | Zinc sulfide nanoparticle-decorated fibre mesh to enable localized H ₂ S-amplified chemotherapy. Chemical Communications, 2020, 56, 4304-4307. | 2.2 | 11 |
| 89 | Electrohydrodynamic coating of metal with nano-sized hydroxyapatite. Bio-Medical Materials and Engineering, 2007, 17, 335-46. | 0.4 | 11 |
| 90 | Theoretical and experimental study of Raman spectra of pre-perovskite PbTiO3. Journal of Applied Physics, 2011, 110, . | 1.1 | 10 |

Xiang Li

| # | Article | IF | CITATIONS |
|-----|---|-----|-----------|
| 91 | Doping and phase transformation of single-crystal pre-perovskite PbTiO3 fibers with TiO6 edge-shared octahedra. CrystEngComm, 2012, 14, 4520. | 1.3 | 10 |
| 92 | Surface plasmon enhanced blue–green photoluminescence from carbon-rich amorphous silicon carbide films. Journal of Alloys and Compounds, 2012, 513, 18-22. | 2.8 | 10 |
| 93 | The nc-Si films with controlled crystal structure and electrical conductivity via the re-crystallization approach. Journal of Non-Crystalline Solids, 2013, 359, 40-45. | 1.5 | 10 |
| 94 | Hydrothermal synthesis and formation mechanism of single-crystal Auivillius Bi4Ti3O12 nanosheets with ammonium bismuth citrate (C6H10BiNO8) as Bi sources. Journal of Crystal Growth, 2017, 476, 31-37. | 0.7 | 10 |
| 95 | A Bifunctional Scaffold for Tissue Regeneration and Photothermal Therapy. Journal of Biomedical Nanotechnology, 2018, 14, 698-706. | 0.5 | 10 |
| 96 | Biodegradable MnFe-hydroxide nanocapsules to enable multi-therapeutics delivery and hypoxia-modulated tumor treatment. Journal of Materials Chemistry B, 2020, 8, 3929-3938. | 2.9 | 10 |
| 97 | <p>VEGF-Modified PVA/Silicone Nanofibers Enhance Islet Function Transplanted in Subcutaneous Site Followed by Device-Less Procedure</p> . International Journal of Nanomedicine, 2020, Volume 15, 587-599. | 3.3 | 10 |
| 98 | EHDA Spraying: A Multi-Material Nano-Engineering Route. Current Pharmaceutical Design, 2015, 21, 3239-3247. | 0.9 | 10 |
| 99 | Catalytic core–shell nanoparticles with self-supplied calcium and H2O2 to enable combinational tumor inhibition. Journal of Nanobiotechnology, 2021, 19, 313. | 4.2 | 10 |
| 100 | Enhanced preferential orientation and electrical property of fluorine-doped SnO2 thin films via barrier layer. Materials Letters, 2014, 122, 143-146. | 1.3 | 9 |
| 101 | Constructing Implantable SrTiO ₃ :Yb,Ho Nanofibers for NIRâ€Triggered and Optically Monitored Chemotherapy. Chemistry - A European Journal, 2017, 23, 2423-2431. | 1.7 | 9 |
| 102 | Silica nanospheres entrapped with ultra-small luminescent crystals for protein delivery. Chemical Engineering Journal, 2017, 330, 166-174. | 6.6 | 9 |
| 103 | KCl-CaCO ₃ nanoclusters armoured with Pt nanocrystals for enhanced electro-driven tumor inhibition. Biomaterials Science, 2022, 10, 376-380. | 2.6 | 9 |
| 104 | Bright blue photoluminescence from the amorphous carbon via surface plasmon enhancement. Optics Express, 2011, 19, 17935. | 1.7 | 8 |
| 105 | Ag-silica composite nanotube with controlled wall structures for biomedical applications. Colloids and Surfaces B: Biointerfaces, 2013, 111, 693-698. | 2.5 | 8 |
| 106 | Dissolution/recrystallization growth of titanate nanostructures by amorphous precursor. Advanced Powder Technology, 2014, 25, 745-751. | 2.0 | 8 |
| 107 | A Reduced Graphene Oxide (rGO)â€Ferroelectrics Hybrid Nanocomposite as High Efficient Visibleâ€Lightâ€Driven Photocatalyst. ChemistrySelect, 2016, 1, 6020-6025. | 0.7 | 7 |
| 108 | Hierarchical nanoclusters with programmed disassembly for mitochondria-targeted tumor therapy with MR imaging. Biomaterials Science, 2021, 9, 8189-8201. | 2.6 | 7 |

XIANG LI

| # | Article | IF | CITATIONS |
|-----|--|-----|-----------|
| 109 | CaCO3-MnSiOx hybrid particles to enable CO2-mediated combinational tumor therapy. Nano Research, 2022, 15, 8281-8290. | 5.8 | 6 |
| 110 | Preparation and characterization of single-crystal multiferroic nanofiber composites. Journal of Alloys and Compounds, 2013, 552, 518-523. | 2.8 | 5 |
| 111 | A flexible smart membrane consisting of GO composite fibres and upconversion MSNs for microRNA detection. Chemical Communications, 2019, 55, 9104-9107. | 2.2 | 5 |
| 112 | NIR light-triggered peroxynitrite anion production <i>via</i> direct lanthanide-triplet photosensitization for enhanced photodynamic therapy. Journal of Materials Chemistry B, 2022, 10, 4501-4508. | 2.9 | 5 |
| 113 | Length-controlled synthesis and the photoluminescence of pre-perovskite PbTiO3 nanofibers. CrystEngComm, 2014, 16, 3567-3572. | 1.3 | 4 |
| 114 | Improved ferromagnetic properties of electrospun NiFe2O4 with tunable morphology: from multiparticle-chain to single-particle-chain. Journal of Nanoparticle Research, 2014, 16, 1. | 0.8 | 4 |
| 115 | Molecular-mediated crystal growth of PbTiO3 nanostructure on silicon substrate. Applied Surface Science, 2011, 257, 9768-9772. | 3.1 | 3 |
| 116 | Generation of biomaterial particles with controlled dimensions via electrospraying. Open Journal of Regenerative Medicine, 2012, 01, 10-17. | 0.5 | 3 |
| 117 | First-principles study of structural stability and elastic property of pre-perovskite PbTiO 3. Chinese Physics B, 2012, 21, 016201. | 0.7 | 3 |
| 118 | Effect of atomic bonding configuration on optical properties of a-Si1â^'xCx:H thin film. Journal of Alloys and Compounds, 2013, 559, 20-23. | 2.8 | 3 |
| 119 | Core–shell SrTiO ₃ :Yb ³⁺ ,Er ³⁺ @mSiO ₂ nanoparticles for controlled and monitored doxorubicin delivery. RSC Advances, 2016, 6, 26280-26287. | 1.7 | 3 |
| 120 | FABRICATION OF NANOPOROUS CHITOSAN MEMBRANES. Nano, 2010, 05, 53-60. | 0.5 | 2 |
| 121 | Polymeric Based Therapeutic Delivery Systems Prepared Using Electrohydrodynamic Processes. Current Pharmaceutical Design, 2016, 22, 2873-2885. | 0.9 | 2 |
| 122 | Amorphous carbon-based films with surface-plasmon-enhanced full-color photoluminescence. Journal of Non-Crystalline Solids, 2012, 358, 1725-1729. | 1.5 | 1 |
| 123 | Hollow nanocapsules of NiFe hydroxides to enable doxorubicin delivery and combinational tumour therapy. Biomaterials Science, 2021, 9, 2598-2607. | 2.6 | 1 |